ANL/CHM/CP--90466 CONF-970138-5

Submitted to:The Second International Symposium on New Materials for Fuel Cells and Modern Battery Systems; to be held in Montreal, Canada on July 6-10, 1997.

NOVEL CARBONACEOUS MATERIALS FOR LITHIUM SECONDARY BATTERIES

Giselle Sandí, Randall E. Winans, Kathleen A. Carrado
and Christopher S. Johnson†.

Chemistry and †Chemical Technology Divisions
Argonne National Laboratory
Argonne, IL 60439. USA.

This work was performed under the auspices of the Office of Basic Energy Sciences, Division of Chemical Sciences, U.S. Department of Energy, under contract number W-31-109-ENG-38.

NOVEL CARBONACEOUS MATERIALS FOR LITHIUM SECONDARY BATTERIES

Giselle Sandí, Randall E. Winans, Kathleen A. Carrado and Christopher S. Johnson†. Chemistry and †Chemical Technology Divisions. Argonne National Laboratory, Argonne, IL 60439. USA.

ABSTRACT

Carbonaceous materials have been synthesized using pillared clays (PILCs) as templates. The PILC was loaded with organic materials such as pyrene in the liquid and vapor phase, styrene in the vapor phase, trioxane, ethylene and propylene. The samples were then pyrolyzed at 700 °C in an inert atmosphere, followed by dissolution of the inorganic template by conventional demineralization methods. X-ray powder diffraction of the carbons showed broad d_{002} peaks in the diffraction pattern, indicative of a disordered or turbostratic system. N_2 BET surface areas of the carbonaceous materials range from 10 to 100 m^2/g. There is some microporosity ($r < 1$ nm) in the highest surface area carbons. Most of the surface area, however, comes from a mixture of micro and mesopores with radii of 2-5 nm. Electrochemical studies were performed on these carbons. Button cells were fabricated with capacity- limiting carbon pellets electrodes as the cathode and metallic lithium foil as the anode. Large reversible capacities (up to 850 mAh/g) were achieved for most of the samples. The irreversible capacity loss was less than 180 mAh/g after the first cycle, suggesting that these types of carbon materials are very stable to lithium insertion and de-insertion reactions.

1. INTRODUCTION

The need for rechargeable high energy power sources has led to a new era of research and development in the battery field. Lithium secondary batteries are among the energy systems of the future because of their low density, high energy and long cycle life. The application of carbonaceous materials for the negative electrode of lithium ion batteries has been investigated intensively in recent years, where the reversible insertion/extraction of lithium into/from a carbon matrix occurs upon charge/discharge instead of the deposition/dissolution of metallic lithium. The dendritic growth of lithium on charging can be avoided and hence the use of carbon anodes can be expected to prolong the cycle life of a whole cell and to improve the safety reliability.

At present, extensive efforts have been dedicated to the research and development of different carbonaceous materials that can deliver high specific capacity, good coulombic efficiency and long cycle life [1-4]. The structure of the carbon is a major factor in the intercalation of lithium, both in how much can be intercalated and at what voltage. So far, a wide variety of carbon materials such as natural graphite, cokes, carbon fibers, non-graphitizable carbon, and pyrolitic carbon have been investigated [5-8]. However, anode materials that show stability and good cycle life are needed for lithium ion batteries.

Surface area and porosity are two important parameters to consider when selecting a carbon

material to be used as an anode electrode. For disordered carbons, both parameters are critical since the irreversible capacity obtained in the first cycle seems to be associated with the surface area (an exfoliation mechanism occurs in which the exposed surface area continues to increase) [9]. Here, we describe the synthesis of disordered carbons where the porosity and surface area are controlled. Tomita et al [10] have shown the preparation of ultrafine carbon tubes by using an aluminum oxide film with uniform channels as a template. Our approach is to use pillared clays (PILCs) as inorganic templates. These modified clays have aluminum oxide supports between the layers that help to prevent the collapse of the layers upon heat treatment. Five organic compounds are used to produce the carbon: pyrene, styrene, trioxane/pyrene, ethylene and propylene. Carbon from pyrene as the precursor is produced by a mechanisms described by Sandí et al. [11] in which the alumina pillars in the clay should act as acid sites to promote condensation similar to the Schöll reaction [12]. Carbon from styrene and trioxane/pyrene are produced by the incorporation of liquid monomer in the PILC, followed by a low temperature polymerization reaction. The polymerization of styrene produces a linear polymer while the trioxane and pyrene reaction produces a condensation polymer similar to phenoplasts. Carbon from ethylene and propylene are synthesized by a mechanism similar to that described by Tomita et al [10] in which the gaseous hydrocarbon is deposited in the PILC layers and subsequently pyrolyzed. After elimination of the inorganic matrix via demineralization, the resulting layered carbons show holes due to the pillaring Al_{13} cluster unit where lithium diffusion may be able to occur. In a previous study of these materials using small angle neutron scattering, Winans and Carrado [13] showed that the diameter of the holes was about 15 Å, which is the approximate size of the Al_{13} pillar. Therefore, lithium should be able to diffuse rapidly through this molecularly porous carbon.

2. EXPERIMENTAL

2.1 Synthesis

The synthesis of the calcined pillared clays (PILCs) has been described in detail elsewhere [11,14]. The calcined PILC was loaded with organic using different procedures described as follows. For pyrene, the pillared clay is stirred in a 0.1 M solution of pyrene (Aldrich, 99%) in benzene (J.T. Baker, 99+% A.C.S.) at room temperature overnight. After filtration, the samples were dark green. Styrene (Aldrich, 99+%) was loaded in the vapor phase. Liquid styrene was heated under a nitrogen flow in a vacuum system. The styrene vapor was carried out to a round bottom flask containing the PILC. The PILC was stirred and heated to 150°C. The PILC turned yellow as the loading process progressed. Trioxane (Aldrich, 99+%) was heated to 70°C. Pyrene was added once the trioxane was completely melted. PILC was then added to the solution and the final sample turned dark green. The reaction was catalyzed by addition few drops of HCl 0.1 M.

The pyrolysis of these samples took place in stainless steel tubes that were purged with nitrogen for several minutes. The tubes were sealed and heated to 700°C for 4 hours. Before opening the tubes, pressure was released by cooling the tubes in liquid nitrogen for approximately 30 minutes.

Ethylene and propylene (AGA, 99.95%) were loaded in the gas phase, where the loading and the pyrolysis processes were done in one step. In this case, a three-zone furnace was used. Quartz boats containing PILC were placed within a quartz tube. The tube was initially flushed with nitrogen for about 3 hours. After that period of time, the gas was switched to propylene or ethylene and the

gas flow was kept about 5 cm^3/min. The temperature of the oven was gradually increased from room temperature (about 5 °C/min) to 700 °C. The oven was then held at that target temperature for 4 hours.

The clay was removed using conventional demineralization methods. The loaded/pyrolyzed PILC was placed in HF, previously cooled at 0 °C to passivate the exothermic reaction, and stirred for about one hour. It was then rinsed to neutral pH and refluxed with concentrated HCl for 2 hours. The sample was washed with distilled water until the pH was > 5 to ensure that there was no acid left. The resultant carbon was oven dried overnight at 120 °C.

2.2 Characterization

X-ray powder diffraction (XRD) patterns of clay precursors and carbons were determined using a Scintag PAD-V instrument, with Cu K_α radiation and a germanium solid-state detector at a scan rate of 0.5° 2Θ/min. N_2 BET surface areas, pore size distributions and thermal isotherms were obtained in an Autosorb 6 instrument (QuantaChrome Comp). Approximately 0.10 g of material was weighed into a pyrex tube and evacuated at 80 mTorr overnight at room temperature. After backfilling with He, the carbon was briefly exposed to air prior to analysis. The static physisorption experiments consisted of determining the amount of liquid nitrogen (LN_2) adsorbing to or desorbing from the material as a function of pressure (P/P_o = 0.025-0.999, increments of 0.025).

2.3 Electrochemical Testing

2.3.1 Electrolyte

The electrolyte was 1M $LiPF_6$ dissolved in 50 vol.% ethylene carbonate (EC) & 50 vol.% dimethylcarbonate (DMC) obtained as a solution from FMC Lithium Division (Gastonia, NC).

2.3.2 Cell assembly

The cell hardware used in the galvanostatic cycling studies was provided by either obtained from either Ray-O-Vac or Eveready Battery Company. The button cells were size 2016 or 1225, and consisted of nickel-plated stainless steel. Cells were assembled in a helium-filled recirculating/purification glovebox (Vacuum/Atmospheres DLX series). Carbon electrode pellets were dried at 80 °C in a vacuum oven inside the glovebox prior to assembly. All cell hardware and separator materials were also rigorously dried in like manner.

The dual electrode configuration in these cells uses metallic lithium as the anode. Cells fabricated are cathode capacity limiting and contain metallic lithium (FMC) foil (0.008"; 0.203 mm) as the anode. Li foil was punched out and cold pressed into a copper screen (0.25 mm thick, Goodfellow Co.), that had been spot-welded into the cap. Electrolyte was added to the lithium surface via a gas-tight syringe. To help wet the lithium surface with the electrolyte one or two drops of 1,2-dimethoxyethane (DME, 99.9+%, Aldrich) was added to the cell. Two pre-punched Celgard 2400 separators (Hoechst-Celanese, Charlotte NC) were placed on top of the wetted lithium foil. More drops of electrolyte and only one drop of DME was added. The cells were allowed to sit undisturbed for about 15 minutes to let the DME evaporate. The carbon electrode pellet was placed against the separator, and a nickel-foil spacer was situated on top of the carbon electrode pellet. The spacer acts as both a current collector and also fills the button cell space, depending on the thickness

of the pellet. The button cell can was placed over the rest of the cell and against the grommet. The cell was loaded onto the die spot for crimp-sealing, and was subsequently pressed to a stack height of 0.061" and 2000 psi. After crimping, the cell voltage was immediately checked for shorts. Those sealed button cells which displayed a good voltage, were transported out of the glovebox for electrochemical testing on an Arbin 2400 station cell cycler.

2.3.3 Pellet Fabrication

Electrodes were prepared using 90% by weight of the carbonaceous materials, 5% by weight of Super S carbon black (Alfa Chemicals), and a binder solution made of polyvinylidene (PVDF, Aldrich, 99+%) dissolved in N-methyl-pyrrolidinone (NMP, Aldrich, 99+%). The Super S carbon black is used to provide electrical contact between carbon grains. An excess of NMP was added to make a slurry. The slurry was oven-dried at 120 °C overnight.

This resulting powder is used to make pellets in carbon-steel dies. About 20-30 milligrams of carbon is put into the die and evened-out with the plunger. The die and plunger are put into the press and are pressed at about 5000 psi. The die is rotated 180 degrees and pressed again at 5000 psi in a one-stroke motion. The die is released from the press and the pellet is carefully removed to avoid fracturing.

3. RESULTS AND DISCUSSION

The XRD pattern of disordered carbons contains only a few diffraction peaks. For cokes and soft carbons heated to near 1000 °C, only the (002) and (004) peaks due to the stacking of the layers and the (100) and (110) two dimensional peaks due to in-plane order can be readily observed. The broad d_{002} peak in the diffraction patterns is indicative of a disordered or turbostratic system [4].

Table I shows the d_{002} and the Lc (layer dimension perpendicular to the basal plane) of the carbons synthesized by the above procedures. The layer dimension Lc is calculated from the 002 reflection peak as described by Kinoshita [15]. The carbons synthesized from propylene and ethylene showed the largest d spacing, whereas pyrene resulted in the shortest of the series, being closer to pyrolytic graphite (d_{002}= 3.35 Å). This implies that the carbons synthesized from ethylene or propylene have a higher degree of disorder than the others previously mentioned. In the first stage of heat treatment at 700°C, the pillared montmorillonite sheet remained intact as evidenced in the XRD pattern (not shown), but the organic precursor is converted to amorphous carbon [16]. The Lc values are in the range of 28 to 34 Å, which indicate that the carbon particles are composed of a spherical assemblage of many quasi-graphitic crystallites [15]. Furthermore, the Lc values obtained for these carbons are comparable with those of the disordered carbons heated at temperatures higher than 1500 °C.

The surface areas of the carbonaceous materials range from 10 to 100 m^2/g. There was some microporosity ($r < 1$ nm) in the highest surface area carbons. Most of the surface area, however, comes from mesopores with radii of 2-5 nm.

Figure 1 shows two examples of LN_2 physisorption isotherms. In the type III isotherm (Figure 2a) there is little adsorption at the beginning. However, once a small island of adsorbate nucleates on the surface, additional adsorption occurs more easily because of the strong adsorbate-adsorbate interactions. Type IV isotherms (Figure 2b) usually occur when multilayers of gas adsorb onto the surface of the pores in a porous solids. Initially, the adsorption looks like a type II or type

III adsorption, but eventually the adsorbed layer gets so thick that it fills up the pores. As a result, no more gas can adsorb and the isotherm saturates [17]. A large hysteresis is observed in the adsorption/desorption isotherm of the carbon sample prepared from pyrene. This hysteresis loop has been observed for samples in which the surface area comes mainly from macropores [18].

Figure 2 shows the coulombic efficiencies calculated as the ratio of the reversible capacity in discharge (or lithium intercalation) over the reversible capacity in charge (or lithium deintercalation) for different coin cells cycled from 0 to 2.5 V at a constant current rate of 18 mA/h. It was not possible to obtain all the lithium back upon intercalation at that voltages, as confirmed by the efficiency values.

Figure 3 shows the variation of discharge specific capacity as a function of cycle number for several coin cells made with the carbonaceous materials mentioned above. This phenomena is due to the well-known irreversible capacity loss effect [4]. This occurrence comes from the formation of a passive layer product due to electrochemical reduction of the electrolyte at the low voltages experienced by the carbon electrodes at end of discharge or intercalation. This reaction contributes greater to the observed discharge capacity in early cycles. After the formation of the passive layer is stabilized, the irreversible capacity then is decreased in subsequent cycles. This capacity cannot be recovered in this cycling voltage range even up to 2.5 V, thus demonstrating that the reduction product is very stable. After 5 to 10 cycles are completed, the rate of specific discharge capacity loss per cycle decreases, even becoming fairly flat for one styrene electrode tested.

Coin cells made with trioxane as the carbon electrode exhibited the largest variation in capacity. One of the possible reasons for this behavior could be the presence of small amounts of oxygen on the carbon surface. A comparative study of the oxygen K-edge near edge x-ray absorption fine structure (NEXAFS) of these carbon samples showed that there is still some oxygen on the surface of the carbon made from trioxane [19]. Guidotti and Johnson [20] found that the presence of CO_2 on the surface of carbon anodes derived from polymethylonitrile divinylbenzene also increased the capacity fade due to irreversible reduction reactions.

Table II summarizes the specific capacity, irreversible capacity in the first cycle and the standard deviation associated with the capacity upon cycling. The irreversible capacity is defined as the difference in capacity between the first and second discharge. Pyrene exhibited the lowest irreversible capacity and capacity fade. However, the performance of these cells in terms of delivered capacity is much higher than graphite (370 mAh/g at 200-300 mV vs. Li) and some other alternative materials currently under study. Carbon K-edge NEXAFS studies showed that these carbon contain hydrogen on the surface [19]. Computer simulations of Li reactions with disordered carbons containing hydrogen [21] have showed that Li readily bonds to a proton-passivated edge carbon resulting in a configuration similar to the organo-lithium molecule $C_2H_2Li_2$. As a result, it provides a second channel for lithium uptake, which only works if the edge carbons are saturated with protons.

While some hysteresis occurs in the discharge-charge voltage profiles [22], these carbon electrodes do deliver very high (675-794 mAh/g) and stable capacities (>50 cycles). Carbon electrodes prepared from the trioxane precursor showed the largest hysteresis effect. We believe that oxygen on the surface is the main cause of this undesirable phenomenon in lithium ion batteries.

4. CONCLUSIONS

It has been shown that carbonaceous materials prepared by the templating method exhibit

more than twice the reversible capacity obtained by graphitic materials. High cycling efficiency and low irreversible capacity are also two factors that make these novel materials good candidates for the new generation of secondary batteries. Control over porosity and surface area are achieved with this unique method. The presence of hydrogen on the surface and edges of the carbon contributes to this high capacity since Li bonds to a proton-passivated edge carbon.

5. ACKNOWLEDGMENTS

This work was performed under the auspices of the U.S. Department of Energy, Office of Basic Energy Sciences, Division of Chemical Sciences, under contract number W-31-109-ENG-38.

6. REFERENCES

1. T. Ohzuku, Y. Iwakoshi, and K. Sawai, *J. Electrochem. Soc.*, **140**, 2490 (1990).
2. M. Mohri, N. Yanagisawa, Y. Tajima, H. Tanaka, T. Mitate, S. Nakajima, M. Yoshida, Y. Yoshimoto, T. Suzuki, and H. Wada, *J. Power Sources*, **26**, 545 (1989).
3. N. Imanishi, H. Kashiwagi, T. Ichikawa, Y. Takeda, O. Yamamoto, and M. Inagaki, *J. Electrochem. Soc.*, **140**, 315 (1993).
4. J. R. Dahn, A. K. Sligh, H. Shi, B. W. Way, W. J. Weydanz, J. N. Reimers, Q. Zhong, and U. von Sacken, in *Lithium Batteries-New Materials, Developments and Perspectives*, G. Pistoia, Editor, p. 1, Elsevier, Amsterdam (1994).
5. A. M. Wilson, and J. R. Dahn, *J. Electrochem. Soc.*, **142**, 326 (1995).
6. K. Tatsumi, N. Iwashita, H. Sakaebe, H. Shioyam, and S. Higuchi, *J. Electrochem. Soc.*, **143**, 716 (1995).
7. R. Kanno, Y. Takeda, T. Ichikawa, K. Nakanishi, and O. Yamamoto, *J. Power Sources*, **26**, 535 (1989).
8. A. K. Sleigh, and U. von Sacken, *Solid State Ionics*, **57**, 99 (1992).
9. B. M. Way, and Ulrich von Sacken, Abstract 830, p. 1020, The Electrochemical Society Extended Abstracts, Vol 96-2, San Antonio, TX, October 6-11, 1996.
10. T. Kyotani, L. F. Tsai, and A. Tomita, *Chem. of Materials*, **8**, 2109 (1996).
11. G. Sandí, R. E. Winans, and K. A. Carrado, *J. Electrochem. Soc.*, **143**, L95 (1996).
12. A. Balaban, and T. Nenitzescu, in *Friedel-Crafts Chemistry*, G. Olah, Editor, vol. 2, p.979, Wiley, New York (1973).
13. R. E. Winans, and K. A. Carrado, *J. Power Sources*, **54**, 11 (1995).
14. G. Sandí, K. A. Carrado, R. E. Winans, J. R. Brenner and G. W. Zajac. *Microporous & Macroporous Materials*. Vol. 431, 1996, in press.
15. K. Kinoshita, *Carbon, Electrochemical and Physicochemical Properties*, p.32, John Wiley & Sons, New York (1988).
16. G. Sandí, R. E. Winans, and K. A. Carrado. American Chemical Society Meeting, Analytical Division, Abstract 40, August 1995, Chicago, IL.
17. S. J. Gregg, and K. S. W. Sing, *Adsorption, Surface Area and Porosity,* Academic Press, London, 1967, p. 121.
18. G. Dyrkacz, personal communication.

19. G. Sandí, K. Song, K. A. Carrado, and R. E. Winans, manuscript in preparation.
20. R. Guidotti, and B. Johnson, *Proc. 11th Ann. Battery Conf. On Applic. And Advances*, 193 (1996).
21. U. Rothlisberger, and M. L. Klein, *J. Am. Chem. Soc.*, **117**, 42 (1995).
22. G. Sandí, R. E. Winans, C. Johnson, P. Stair, and C. Lin, Abstract 861, p.1061, The Electrochemical Society Extended Abstracts, Vol 96-2, San Antonio, TX, October 6-11, 1996.

DISCLAIMER

TABLE I: CRYSTALLINE PARAMETERS OF CARBONS PREPARED FROM DIFFERENT PRECURSORS

Carbon from	d_{002} spacing Å	Lc Å
Pyrene	3.42	32
Styrene	3.50	28
Propylene	3.56	28
Ethylene	3.58	30
Trioxane/pyrene	3.49	34

TABLE II: EFFECT OF DIFFERENT CARBON PRECURSORS ON THE PERFORMANCE OF LI/CARBON COIN CELLS

Carbon from	Average specific capacity, mAh/g	Standard deviation, mAh/g	Irreversible capacity, mAh/g
Pyrene	720	60	62
Styrene	730	45	177
Propylene	794	91	180
Trioxane/pyrene	675	75	165

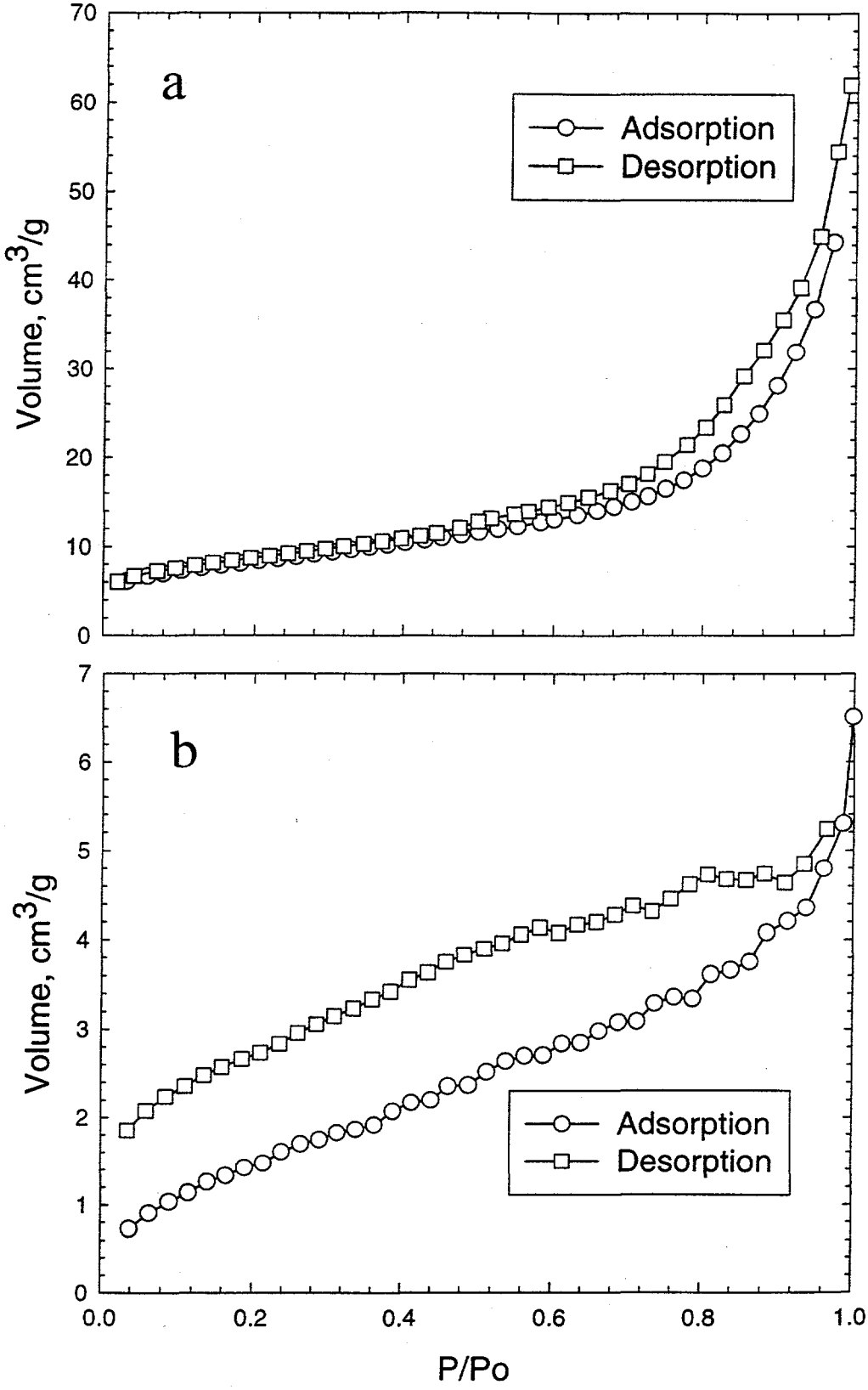

FIGURE 1. NITROGEN ADSORPTION-DESORPTION ISOTHERM OF CARBON SAMPLES FROM A) PROPYLENE AND B) PYRENE, USING PILCS

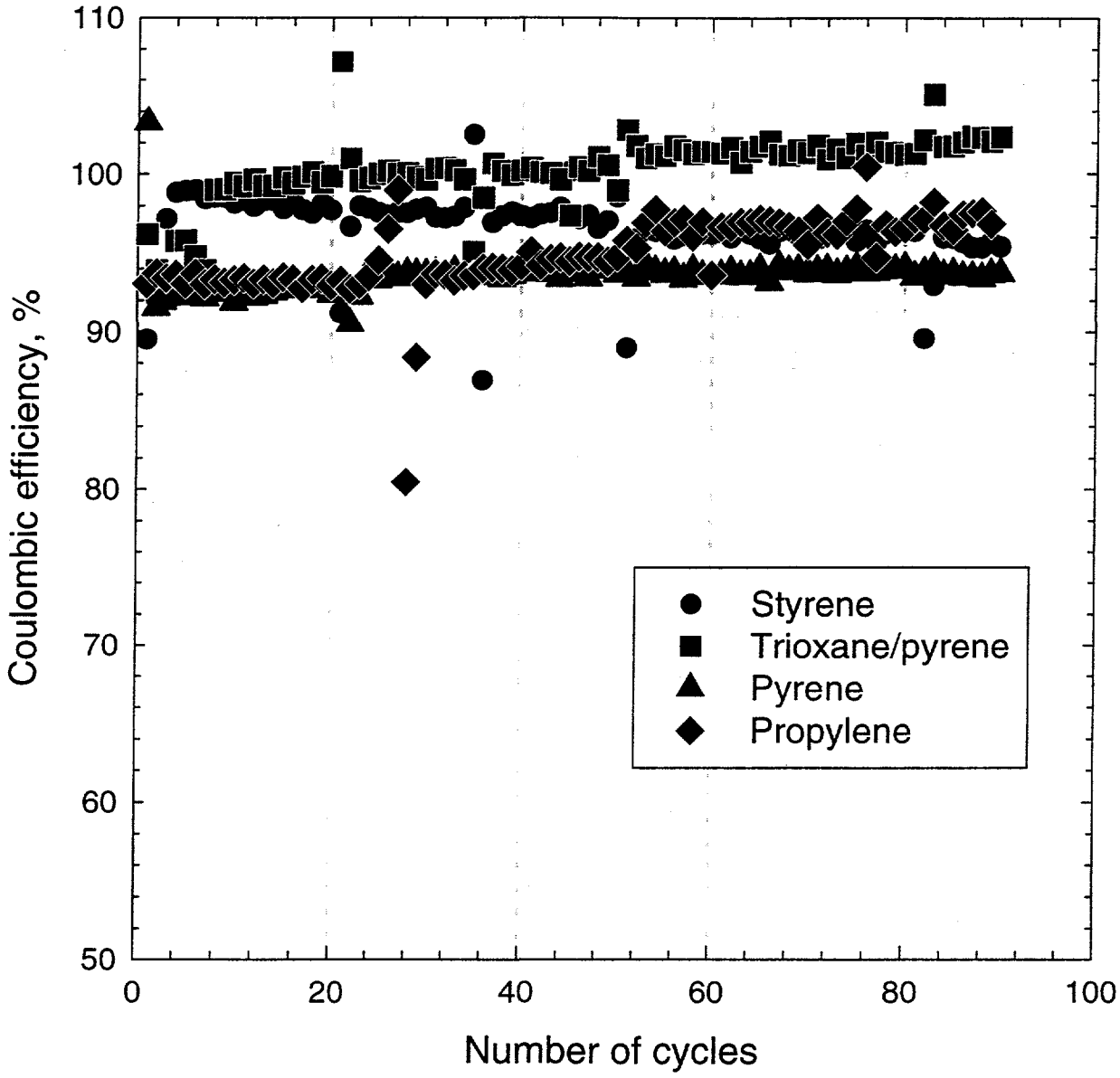

FIGURE 2. COULOMBIC EFFICIENCIES OBTAINED FOR CARBON/LI COIN CELLS CYCLED BETWEEN 0 AND 2.5 V.

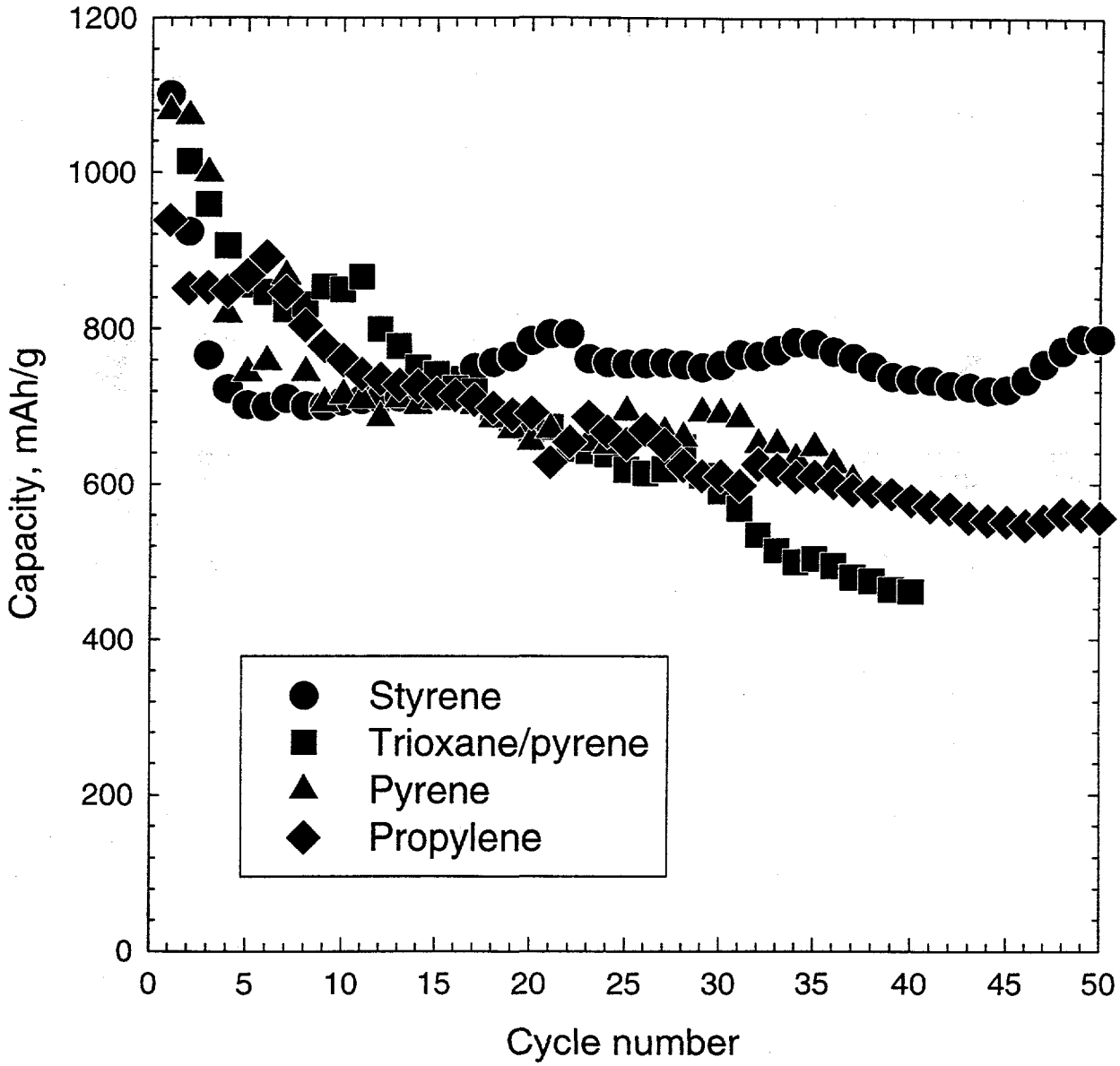

FIGURE 3. VARIATION OF SPECIFIC CAPACITY AS A FUNCTION OF CYCLE NUMBER FOR VARIOUS LI/CARBON COIN CELLS CYCLED FROM 0 TO 2.5 V